

Tuning InAs quantum dots for high areal density and wideband emission

C. Y. Ngo,^{a)} S. F. Yoon, and W. J. Fan
*School of Electrical and Electronic Engineering, Nanyang Technological University,
 Nanyang Avenue, Singapore 639798, Republic of Singapore*

S. J. Chua
*Faculty of Engineering, Institute of Materials Research and Engineering,
 3 Research Link, Singapore 117602, Republic of Singapore*

(Received 5 December 2006; accepted 6 February 2007; published online 12 March 2007)

The authors report the effect of growth temperature and monolayer coverage on areal density and photoluminescence spectral width of InAs quantum dot (QD). Areal density and spectral width were found to be strongly dependent on growth temperature and monolayer coverage, respectively. Upon proper tuning, both high areal density and large photoluminescence spectral width were obtained. Areal density of $1.5 \times 10^{11} \text{ cm}^{-2}$ is four times higher than those previously reported, while spectral width of 136 nm is the broadest spectral width obtained without any forms of band gap engineering. These results will contribute to an improvement in the performance of QD superluminescent diode. © 2007 American Institute of Physics. [DOI: 10.1063/1.2713148]

Superluminescent diodes (SLDs) are important broadband light sources for applications in optical measurement systems such as optical gyroscopes and sensors,¹ short and medium distance optical communication systems,² and biomolecular imaging based on optical coherent tomography.³ For such applications, quantum dot (QD) system is proposed to be the best candidate for ultrawide spectrum due to inhomogeneous broadening of its gain spectrum as a result of the size nonuniformity in self-assembled quantum dots.⁴ In particular, high output power and large optical bandwidth are key figures of merit for QD-SLDs. Common methods to increase the operating power include tilted-stripe structure,⁵⁻⁷ antireflection coating,⁸ or multiple QD layers,⁹ while spectral width is increased by growing chirped QD structure^{5,6,10} or utilizing emission from the excited states (ES).⁶ As such, QD-SLD with high continuous wave output power of 200 mW was demonstrated at room temperature using a tilted-stripe structure with multiple QD layers,⁹ while large spectral width of 121 nm was demonstrated with the use of chirped QD structure and utilizing ES emission.⁶ However, due to the small photoluminescence (PL) spectral width contributed by each QD layer, chirped QD structure must be properly designed. Otherwise, the PL spectral will exhibit intensity peaks and valleys.^{5,6}

For high power broadband applications, both high dot areal density and large size inhomogeneity are desired.⁴ High dot areal density ($\sim 1 \times 10^{11} \text{ cm}^{-2}$) will improve the optical output power of QD-SLDs since, unlike QD lasers, emission from QD-SLDs is contributed by QDs of all sizes. Size inhomogeneity in small QDs, as compared to large QDs, is preferred as this will result in larger energy range,¹¹ implying a wider spectral width. In fact, size inhomogeneity of $\sim 10\%$ occurs naturally in self-assembly QD growth,¹² and it was reported that typical In(Ga)As QDs with size inhomogeneity of 10% give a PL spectral width of 60–80 meV. The fact that this energy range is similar to the PL results^{5-7,13} seems to imply that no effort was made to increase the QD size inhomogeneity within each QD layer. Furthermore, as

reported,^{7,13,14} the areal density of the InAs QDs only ranges from 1.0×10^{10} to $3.5 \times 10^{10} \text{ cm}^{-2}$. Hence, there is no report on optimization of the InAs QD active layers for SLD applications, i.e., to increase both the QD areal density and PL spectral width.

In the present work, we investigated the effects of growth temperature (T_g) and monolayer coverage (θ_c) on the areal density and PL spectral width of the InAs QD samples. As such, the T_g investigated were 450, 480, and 510 °C, while the θ_c investigated were 2.0, 2.5, and 3.0 ML. Our samples were grown using solid-source molecular beam epitaxy. A 250-nm-thick GaAs buffer layer was grown on semi-insulating GaAs (001) substrate before growing θ_c of InAs QDs at substrate temperature of T_g . The QDs were then capped with 5 nm of $\text{In}_{0.15}\text{Ga}_{0.85}\text{As}$ strain reducing layer to tune the ground state emission to around 1.3 μm . This was followed by a 40-nm-thick GaAs spacer layer to decouple the electronic and strain effects of the QD layers,^{15,16} before repeating the above growth sequence for another layer of capped InAs QDs with the same monolayer coverage as the first layer. Finally, a layer of uncapped InAs QDs of the same monolayer coverage was grown for atomic force microscopy (AFM) characterization. The PL properties of the InAs QD samples were measured at room temperature (RT) using the 5145 Å line of an Ar^+ laser. The PL signals were detected using a liquid nitrogen cooled Ge detector in conjunction with a standard lock-in technique.

Figure 1 shows the InAs QD areal density (10^{10} cm^{-2}) and RT-PL spectral width as a function of growth conditions. The trend of variation is divided into regions I and II, namely, θ_c variation at 450 °C and T_g variation at 2.0 ML, respectively. One can see that lower T_g leads to higher dot areal density. Hence, regardless of monolayer coverage, the dot areal density obtained at 450 °C is still higher ($> 7 \times 10^{10} \text{ cm}^{-2}$) than that grown at higher T_g . As reported,¹⁷ the increase in dot areal density at low T_g is due to reduction of the adatom migration length. Hence, impinging adatoms is more likely to form new sites on the surface instead of combining with existing dots. Furthermore, we see an increase in PL spectral width following a decrease in the

^{a)}Electronic mail: ngoc0003@ntu.edu.sg

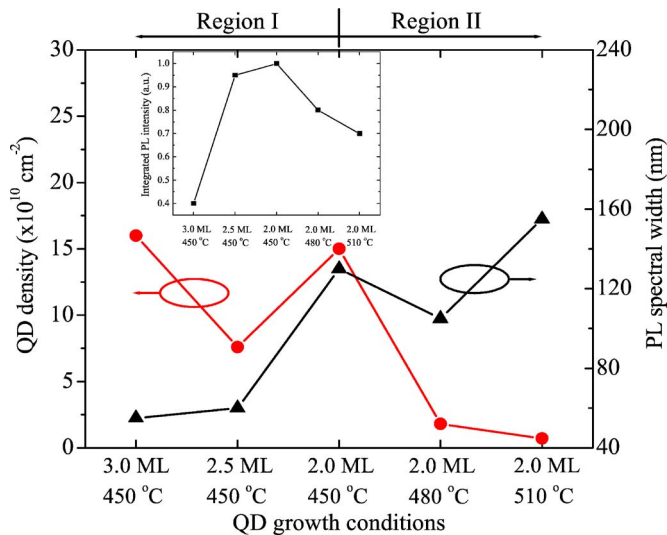


FIG. 1. (Color online) QD areal density (10^{10} cm^{-2}) and RT-PL spectral width as a function of growth conditions. (Inset) Integrated PL intensity as function of growth conditions.

monolayer coverage. Again, note that regardless of growth temperature, the spectral width of the PL spectra at 2.0 ML coverage is still larger ($>100 \text{ nm}$) than that grown at higher θ_c . As reported by Joyce *et al.*,¹⁸ 2.0 ML coverage provides insufficient material for the InAs QDs to reach its mature size. Hence, the large PL spectral width is due to the low InAs monolayer coverage, leading to a large number of QDs in various stages of development and consequently resulting in large QD size variation, as reflected by the wide PL spectral width.

The inset in Fig. 1 presents the integrated PL intensity as function of growth conditions, while Fig. 2 shows the RT-PL spectra and AFM images (as insets) of the InAs QD samples grown at (a) 3.0 ML, 450 °C and (b) 2.0 ML, 510 °C. Hence, while high dot areal density can be obtained at low T_g regardless of monolayer coverage, integrated PL intensity decreases and the number of large islands with width of $\sim 100 \text{ nm}$ increases following the increase in θ_c [as shown in inset of Fig. 2(a)]. As reported,¹⁸ transmission electron microscopy studies have shown the presence of dislocations within the large islands. Hence, these islands are nonradiative and act as a sink for photogenerated carriers, thus degrading the PL efficiency. On the other hand, while large spectral width (implying large size nonuniformity) can be obtained from low InAs coverage, the areal density decreases significantly following the increase in T_g . This is due to the exponential increase in In desorption rate at high growth temperature,¹⁹ hence giving rise to the sharp decrease in the areal density, as observed in Fig. 1 and the AFM image in inset of Fig. 2(b). The corresponding decrease in the integrated PL intensity is expected since, as mentioned above, low areal density ($\sim 0.7 \times 10^{10} \text{ cm}^{-2}$) is detrimental to the output power of QD-SLDs. While extraction of the actual dot height from AFM is relatively straightforward, this is not so for the dot width (lateral size) due to convolution effects between the AFM tip and the dot. In this work, all AFM image widths have been corrected to obtain the actual widths (lateral size).²⁰ The size nonuniformities²¹ for the insets of Figs. 2(a) and 2(b) are calculated to be 12.3% and 19.4%, respectively. It should be noted that the large islands in the inset of Fig. 2(a) are excluded from the nonuniformity cal-

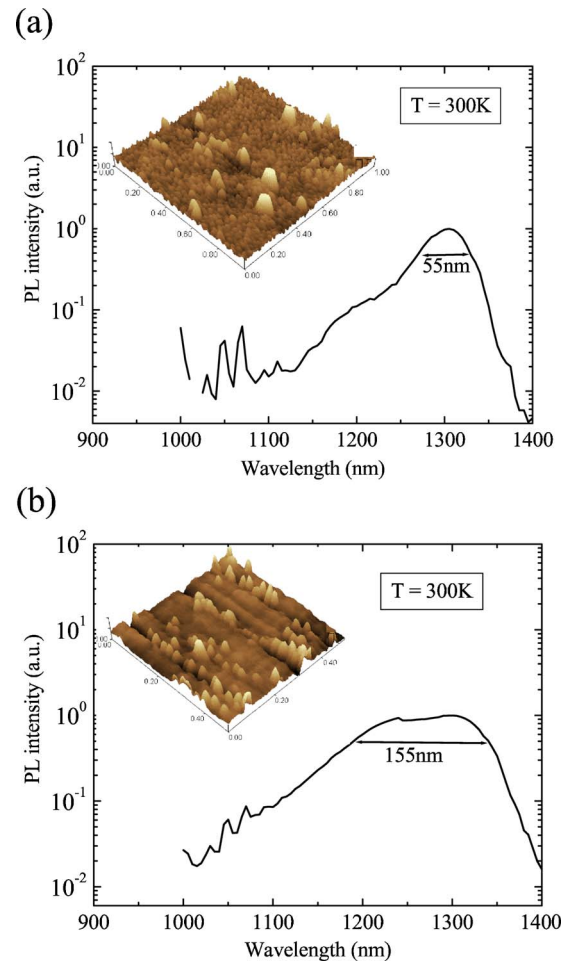


FIG. 2. (Color online) RT-PL spectra of the InAs QD samples grown at (a) 3.0 ML, 450 °C and (b) 2.0 ML, 510 °C. The corresponding spectral widths are indicated. (Inset) Corresponding AFM images of the InAs QD samples. Note the presence of large islands with width of $\sim 100 \text{ nm}$ in the AFM image in (a).

culations since they are nonradiative. The increase in size nonuniformity following the decrease in monolayer coverage is expected and can be inferred from the spectral widths of the PL spectra in Fig. 2.

As seen from Fig. 1, InAs QD areal density is strongly dependent on the growth temperature, while the size nonuniformity (thus spectral width of the PL spectrum) is strongly dependent on the monolayer coverage. This implies the ability to tune the dot areal density and size nonuniformity separately by changing the InAs QD growth conditions. Hence, using suitable monolayers coverage and growth temperature, one can obtain high dot areal density and large spectral width. As depicted in Fig. 1, this is realized for InAs QD sample grown at 2.0 ML and 450 °C, and Fig. 3 shows the (a) AFM image and (b) RT-PL spectra of the sample under various fractions of excitation power. The QD areal density obtained from the AFM image was $1.5 \times 10^{11} \text{ cm}^{-2}$ and the size nonuniformity was calculated to be 19.0%. This areal density is approximately four times higher than those previously reported^{7,13,14} and is expected to contribute to the higher output power of QD-SLDs. Comparison of the PL spectrum at $1.0P_0$ with that at $0.25P_0$ suggests that the broadband emission is contributed by a convolution of various ground and excited state emissions. This explains the presence of the shorter wavelength peaks at higher excitation

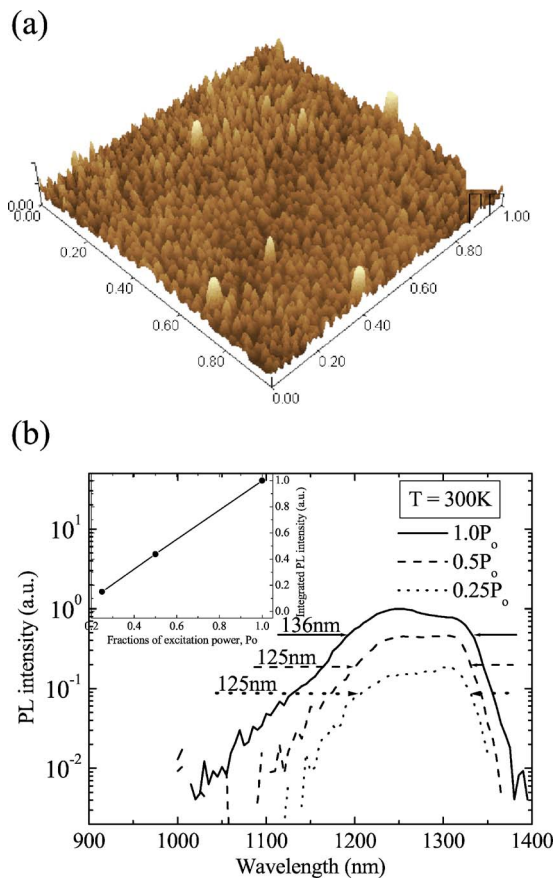


FIG. 3. (Color online) (a) AFM image and (b) RT-PL spectra of InAs QD sample grown at 2.0 ML, 450 °C under various fractions of excitation power. The initial excitation power is P_0 . The corresponding spectral widths are indicated. (Inset) Integrated PL intensity as function of excitation power.

power. Due to the small size variation around the average QD size, a continuous intensity profile with spectral width of 125 nm is observed even at $0.25P_0$. This broad spectrum is advantageous since ground state emission from small QDs will overlap with emission from larger QDs. Good quality InAs QD growth can be inferred from the near-unity gradient of the integrated PL intensity as function of excitation power (as depicted in the inset of Fig. 3), suggesting that almost all photogenerated carriers contribute to the PL emission. At full excitation power, the InAs QD sample exhibits a spectral width of 136 nm, spanning from 1195 to 1331 nm. The intensity profile is relatively smooth, and there is no dip in the PL intensity as compared to those reported.^{5-7,13} This is the broadest spectral width ever reported in samples without any forms of band gap engineering.^{5,6,10}

In conclusion, we have investigated the effect of InAs QD growth temperature and monolayer coverage on the areal

density and size nonuniformity of InAs QDs. Under conditions of InAs QD growth temperatures at 450, 480, and 510 °C and monolayer coverages at 2.0, 2.5, and 3.0 ML, the InAs QD areal density was found to be strongly dependent on the growth temperature while the size nonuniformity was found to be strongly dependent on the monolayer coverage. With proper tuning of growth temperature and monolayer coverage, we had achieved both high areal density ($1.5 \times 10^{11} \text{ cm}^{-2}$) and large RT-PL spectral width (136 nm). These results will contribute to an improvement in the performance of the current QD-SLDs.

The authors greatly acknowledge the discussions with Sun Zhongzhe. This project is partially supported by funding under the A*STAR Graduate Scholarship program.

¹W. K. Burns, C. L. Chen, and R. P. Moeller, *J. Lightwave Technol.* **LT1**, 98 (1983).

²E. J. Friebele and A. D. Kersey, *Laser Focus World* **30**, 165 (1994).

³T. H. Ko, D. C. Adler, and J. G. Fujimoto, *Opt. Express* **12**, 2112 (2004).

⁴Z. Z. Sun, D. Ding, Q. Gong, W. Zhou, B. Xu, and Z. G. Wang, *Opt. Quantum Electron.* **31**, 1235 (1999).

⁵I. K. Han, H. C. Bae, W. J. Cho, J. I. Lee, H. L. Park, T. G. Kim, and J. I. Lee, *Jpn. J. Appl. Phys.* **44**, 5692 (2005).

⁶L. H. Li, M. Rossetti, A. Fiore, L. Occhi, and C. Velez, *Electron. Lett.* **41**, 41 (2005).

⁷D. C. Heo, S. J. Dong, W. J. Choi, J. I. Lee, J. C. Jeong, and I. K. Han, *Jpn. J. Appl. Phys.* **42**, 5133 (2003).

⁸T. L. Paoli, R. L. Thornton, R. D. Burnham, and D. L. Smith, *Appl. Phys. Lett.* **47**, 450 (1985).

⁹Z. Y. Zhang, Z. G. Wang, B. Xu, P. Jin, Z. Z. Sun, and F. Q. Liu, *IEEE Photonics Technol. Lett.* **16**, 27 (2004).

¹⁰I. K. Han, D. C. Heo, J. D. Song, I. Lee, and J. I. Lee, *J. Korean Phys. Soc.* **45**, 1193 (2004).

¹¹C. Y. Ngo, S. F. Yoon, W. J. Fan, and S. J. Chua, *Phys. Rev. B* **74**, 245331 (2006).

¹²Y. Ebiko, S. Muto, D. Suzuki, S. Itoh, K. Shiramine, and T. Haga, *Phys. Rev. Lett.* **80**, 2650 (1998).

¹³S. K. Ray, K. M. Groom, H. Y. Liu, M. Hopkinson, and R. A. Hogg, *Jpn. J. Appl. Phys.* **45**, 2542 (2006).

¹⁴C. Velez, L. Occhi, M. Rossetti, L. H. Li, and A. Fiore, *Proc. SPIE* **5690**, 214 (2005).

¹⁵G. S. Solomon, J. A. Trezza, A. F. Marshall, and J. S. Harris, *Phys. Rev. Lett.* **76**, 952 (1996).

¹⁶P. Howe, E. C. Le Ru, E. Clarke, R. Murray, and T. S. Jones, *J. Appl. Phys.* **98**, 113511 (2005).

¹⁷S. Franchi, G. Trevisi, L. Seravalli, and P. Frigeri, *Prog. Cryst. Growth Charact. Mater.* **47**, 166 (2003).

¹⁸P. B. Joyce, T. J. Krzyzewski, G. R. Bell, and T. S. Jones, *Phys. Rev. B* **64**, 235317 (2001).

¹⁹C. T. Foxon and B. A. Joyce, *J. Cryst. Growth* **44**, 75 (1978).

²⁰Using $w_d = \sqrt{w_i^2 - 8r_i h}$, where w_d , w_i , r_i , and h are the actual dot width, AFM image width, radius of curvature of the tip, and dot height, respectively. Derivation of the formula is included in the Appendix of *J. Appl. Phys.* (unpublished).

²¹Nonuniformity is defined as the ratio of the standard deviation of the sample size to the average of the sample size.